

REDOUANE OUAFI¹
ANASS OMOR¹
YOUNES GAGA²
MOHAMED AKHAZZANE¹
MUSTAPHA TALEB¹
ZAKIA RAIS¹

¹Engineering Laboratory of
Organometallic, Molecular
Materials and Environment, Faculty
of Science Dhar El Mahraz, Sidi
Mohamed Ben Abdellah University,
Route d'immouzer, Fez, Morocco

²Laboratory of Biotechnology,
Ecology and Preservation of
Natural Resources, Faculty of
Science, Dhar El Mahraz, Sidi
Mohamed Ben Abdellah University,
Route d'immouzer, Fez, Morocco

SCIENTIFIC PAPER

UDC 544.723:58:66

PINE CONE POWDER FOR THE ADSORPTIVE REMOVAL OF COPPER IONS FROM WATER

Article Highlights

- Valorisation of a natural waste in the treatment of copper ions from aqueous solutions
- The adsorption process was successfully represented by pseudo-second-order kinetic model
- Langmuir isotherm model describes the adsorption of Cu(II) ions onto pine cone powder
- The functional group study set the role of hydroxyl, carboxyl and phenolic groups in metal binding
- Pine cone powder can be used as adsorbent for the removal of copper ions from aqueous solution

Abstract

This research investigates the adsorption potential of pine cone powder (PCP) for the removal of copper ions (Cu(II)) from aqueous solutions. The process of adsorption was reasonably fast, completed within a time of 60 min. The pseudo-second order kinetic model describes properly the Cu(II) adsorption by PCP. The adsorbent was characterised by various instrumental techniques and batch experiments were conducted to investigate the effect of PCP dose, solution pH, particle size and initial Cu(II) concentration on adsorption efficiency. Optimum Cu(II) removal occurred at a slightly acidic pH, with a particle size less than 100 µm. The effective PCP dose was estimated to be 36 g L⁻¹. The increase in the initial concentration of Cu (II) was accompanied by a reduction in the rate of its reduction by almost half. The Langmuir model was the best fitting isotherm with a maximum adsorption capacity of 9.08 mg g⁻¹. The thermodynamic parameters values showed that the Cu(II) adsorption was a spontaneous and endothermic process. The results of this research suggest that Cu(II) could be removed through an environmentally friendly process using PCP as low-cost natural waste.

Keywords: copper ion removal, isotherms, kinetic, natural waste, pine cone powder, water treatment.

The growth of industrial activity has resulted in the discharge of large quantities of pollutants including dyes, phenols, oil, toxic salts and heavy metals. The toxic nature of these contaminants constitutes a severe threat to human health and the whole biological system. Consequently, their treatment remains a topic of scientific interest [1]. Among these pollutants, copper is one of the most prevalent heavy

metal pollutants in the environment because of its extensive use in many industries. It is used in electronics, construction, electroplating, surface treatment and brass industry. At high levels, chronic overexposure to copper can lead to various health effects on human beings, including liver and kidney damage, Wilson's disease and carcinogenicity [2,3]. Thus, because of its toxic properties at high levels, copper-contaminated water should be treated before its discharge in the environment.

In recent decades, a growing interest in natural, available and low-cost adsorbents has been observed, and they have been extensively used for heavy metal and other pollutant removal [4]. Therefore, various materials have been investigated as adsorbents

Correspondence: R. Ouafi, Sidi Mohamed Ben Abdellah University, Route d'immouzer, B.P 2626, Fez, Morocco.

E-mail: redouane.ouafi@usmba.ac.ma

Paper received: 1 January, 2020

Paper revised: 4 December, 2020

Paper accepted: 12 January, 2021

<https://doi.org/10.2298/CICEQ200101001O>

to remove different types of pollutants from wastewater. These materials include mineral materials, synthetic organic materials, agriculture wastes, industrial by-products and natural residues [5-7].

One of the most important challenges that face researchers in adsorption investigations is the selection of favourable types of biomass among numerous materials. Sawdust has been widely studied for its property to remove pollutants from wastewater. It is considered as an economic, efficient, sustainable and green process. It was hence extensively reported as a low-cost potent remedial tool [8].

In parallel with the ongoing research for cheaper, viable and probable adsorbents, the efficiency of pine cones for Cu(II) removal has been investigated. Further, it will be a step forward in exploring the possibility of using waste biomass to remove pollutants from wastewater. Pine cone is abundant in nature, requires little processing and represents an unused resource. It contains various organic compounds such as cellulose, hemicellulose and lignin, which contain several groups that would attach compounds through different mechanisms [9-12]. Preliminary research have previously shown the potential use of pine cones in the treatment of various compounds [13-15]. However, very few works have reported its applicability for Cu(II) removal [16-18]. The aim of this work was to deepen the studies of different depollution parameters influencing the use of this natural waste in the treatment of wastewater. Thus, a local pine cone, collected from the peri-urban forests in Fez, Morocco, was investigated for its application for the treatment of Cu(II) from aqueous solutions. The kinetics were studied by applying pseudo-first order, pseudo-second order, intraparticle diffusion and Elovich kinetics models. The effect of the experimental parameters such as pH of solutions, adsorbent dose, initial metal concentration, and contact time on the adsorption efficiency were inspected. The characterisation of the products before and after the reaction was carried out by using physicochemical technique. Langmuir, Freundlich, Redlich-Peterson and Dubinin-Radushkevich isotherm models were used to analyse experimental data of Cu(II) adsorption by PCP. Thermodynamic analysis was used to describe the nature of the process.

MATERIALS AND METHODS

Adsorbent material preparation

The pine cones (*Pinus halepensis*) were collected from the peri-urban forests in Fez, Morocco. The cone scales were removed and then rinsed

extensively with distilled water. The materials were oven-dried at 60 °C for 48 h. The above dried natural waste was ground to a fine powder. The resulting pine cone powder (PCP) was sieved and stored for experimental purposes.

Preparation of aqueous metal ions solutions

The solutions of Cu(II) were prepared by dissolving 3.927 g of CuSO₄·5H₂O in deionised water obtained by Barnstead EASYPure II system to achieve a concentration of 1000 mg L⁻¹. Experimental solutions of the desired concentrations of metal ions were prepared by diluting the stock solution in deionised water. The pH of the solutions was adjusted using 0.1 N HCl and 0.1 N NaOH to achieve the desired values. The pH measurements were performed using a Hanna pH-meter model HI 2221.

Metal concentration analysis

The metal concentration analysis was determined using inductively coupled plasma atomic emission spectroscopy (ICP-AES) model Activa from Horiba Jobin-Yvon, equipped with an argon plasma, cyclonic chamber and concentric nebuliser.

Physicochemical characterisation

The pH and the electrical conductivity (EC) were determined by placing 1 g of PCP in contact with 100 mL of distilled water and then shaken for 24 h. After filtering the suspension, the pH and EC values of the filtrate were measured using a Hanna pH-meter model HI 2221. The point of zero charge of PCP (pH_{pzc}) was determined by solid addition method in our previous research [19].

The specific surface area (S_{BET}) was measured using a Gemini VII 2390t surface area analyser (Micromeritics Instruments Corp.) The value of S_{BET} was determined from the N₂ adsorption isotherms by applying the Brunauer-Emmett-Teller (BET) equation at a relative pressure range of 0.05-0.30 and an average area per molecule of N₂ in a completed monolayer (σ_m) of 0.162 nm².

Scanning electron microscopy (SEM) was carried out by a FEI-Quanta 200 environmental scanning electron microscope under a vacuum of 90 Pa, an accelerating voltage (HV) of 15 kV and a working distance (WD) of 9.8 mm.

The Fourier-transform infrared spectroscopy (FTIR) was recorded using Bruker FTIR spectrophotometer model Vertex 70, in the range of 400-4000 cm⁻¹, using ATR mode; 16 scans were accumulated at a resolution of 4 cm⁻¹.

The X-ray diffraction pattern (XRD) of the sample was obtained using a Panalytical X'Pert Pro

X-ray diffractometer equipped with a CuK α monochromatic source (1.54 Å), operating at a voltage of 40 kV and a filament current of 40 mA. The diffraction pattern was recorded from 5 to 40° (2θ) at a scan step time of 90.17 s.

The thermal gravimetric analysis (TGA) and the differential thermal analysis (DTA) were performed using a Shimadzu DTG-60H instrument under air atmosphere, with a heating rate of 20 °C/min from 27 to 1000 °C. The sample mass introduced was 11.16 mg.

Kinetic study

The adsorption kinetic was conducted using the batch method. The experiments were carried out in 100 mL Erlenmeyer flasks containing 1.8 g of adsorbent mixed with 50 mL of Cu(II) solution at an initial concentration of 100 mg L⁻¹, a pH of 5.3 and a temperature equal to 25 °C. The flasks were agitated at a constant speed of 200 rpm in a shaker incubator (Cleaver Scientific Ltd). After specified intervals of time from 5 to 180 min, the solutions were collected and filtered using a 0.22 µm filter paper. The Cu(II) concentrations were determined using ICP-AES.

The amounts of metal ions adsorbed on the adsorbent phase q_t (mg g⁻¹) were calculated from the following expression:

$$q_t = \frac{(C_0 - C_t)V}{m} \quad (1)$$

where C_0 and C_t are the initial metal ions concentration and concentration at a defined time (mg L⁻¹), V is the solution volume (L) and m is the mass of the adsorbent (g).

Pseudo-first-order (PFO) [20], pseudo-second-order (PSO) [21], the intraparticle diffusion [22] and Elovich [23] model, in linearised form, were selected to examine the ability of these types of kinetic models to describe adsorption of Cu(II) by PCP.

Batch adsorption experiments

The adsorption experiments in batch modes were carried out by bringing into contact in 100 ml flasks a determined quantity of adsorbents, with 50 mL of a synthetic solution of Cu(II) at the desired concentration. The flasks were stirred in a shaker incubator (Cleaver Scientific Ltd.) at the required temperature and time. After sufficient contact time, allowing the adsorption to reach equilibrium, the solutions were collected and filtered. Afterwards, the Cu(II) concentrations in the filtrate were determined.

The amount of adsorbate per gram of adsorbent denoted q_e (mg/g) was calculated from the following expression:

$$q_e = \frac{(C_0 - C_e)V}{m} \quad (2)$$

The Cu(II) elimination rate R (%) was defined by:

$$R = 100 \frac{C_0 - C_e}{C_0} \quad (3)$$

where C_e is the residual metal ions concentration measured at equilibrium (mg L⁻¹).

Effect of adsorption parameters

The effect of adsorbent dose was determined by varying the amount of PCP from 0.1 to 2.8 mg, the measured amount of PCP was stirred in a 100 mL Erlenmeyer flask with 50 mL of 100 mg L⁻¹ Cu(II) at 25 °C.

The effect of pH on the adsorption process was examined maintaining the described batch experiments and varying the pH of the solution from 2 to 8 in a solution of initial Cu(II) concentration of 100 mg L⁻¹ with adsorbents mass of 1.8 g at 25 °C.

The effect of particle size of PCP was examined through different particle size powders (50, 100, 200, 300 and 800 µm) with a solution of initial Cu(II) concentration equal to 100 mg L⁻¹, an adsorbent mass of 1.8 g, temperature of 25 °C and a solution pH of 5.3.

The effect of metal concentration on Cu(II) elimination rate was examined by varying the Cu(II) concentration from 20 to 500 mg L⁻¹ with an adsorbent mass of 1.8 g, particle size powder of 50 µm and temperature equal to 25 °C. The pH of the solution remained at 5.3.

Equilibrium isotherm models

Langmuir [24], Freundlich [25], Dubinin-Radushkevich [26] and Redlich-Peterson [27] models were used to describe the distribution of metal ions between liquid and solid phases. To calculate the parameters of isotherm models accurately in batch experiments, the use of the nonlinear method rather than the linear method has been advised by numerous researchers [28]. Nonlinear optimisation is a mathematically rigorous method to determine the parameters of the adsorption model using the original form of the equation. Accordingly, the isotherm models were fitted through the Levenberg-Marquardt algorithm using OriginPro software.

Thermodynamic study

The thermodynamic parameters were investigated at 298, 313, 323 and 333 K. The standard free energy changes (ΔG°), standard enthalpy change (ΔH°) and standard entropy change (ΔS°) were calculated according to the following equations [29]:

$$\Delta G = -RT \ln K_c \quad (4)$$

$$\Delta G = \Delta H - T \Delta S \quad (5)$$

$$\ln K_c = -\frac{\Delta H}{R} \frac{1}{T} + \frac{\Delta S}{R} \quad (6)$$

where R is the universal gas constant ($8.3144 \text{ J mol}^{-1} \text{ K}^{-1}$), T is the absolute temperature (K), and K_c the equilibrium constant.

According to previous research [30-32], the equilibrium constant K_c could be derived from the Langmuir constant using the following equation:

$$K_c = 63.54 \times 55.5 \times 1000 K_L \quad (7)$$

where the $55.5 (\text{mol L}^{-1})$ is the number of moles of pure water per litre, $63.54 (\text{g mol}^{-1})$ is the molecular weight of adsorbate (copper), $1000 (\text{g L}^{-1})$ is the value for the density of water and K_L is the Langmuir constant (L mg^{-1}).

Error functions

The goodness of the experimental data fit to the proposed kinetic and isotherm models was evaluated by the coefficient of determination, which is also known as R -squared (R^2) and by Adj. R -squared (R_{adj}^2). In general, the closer R^2 and R_{adj}^2 to 1, the better the fitted line fits the data. Their values are between 0 and 1.

RESULTS AND DISCUSSION

Characteristics of PCP

SEM analysis

The irregularity, roughness and heterogeneous texture characterised the raw PCP surface (Figure 1a). These surface distortion gives a favourable condition for the retention of Cu(II) between the interstices. These characteristics were also reported by other research [33,34]. The inspection of SEM images after Cu(II)-loaded PCP (Figure 1b) revealed no obvious difference compared to the raw PCP material.

FTIR analysis

The FTIR spectra of both raw PCP and PCP after metal adsorption given in Figure 2 present various bands characteristic of the chemical structure of cellulose. The FTIR spectral analysis of raw PCP was interpreted in a detailed manner in our previous investigation [19]. Compared to raw PCP spectrum, spectrum of Cu(II)-loaded PCP shows a decrease in the intensity of the major infrared bands.

The band intensity of the OH groups decreased significantly and shifted from 3301 to 3350 cm^{-1} after Cu (II) adsorption suggesting the possible formation of complexes between OH groups and metal loaded. The shift in the bands from 1718 to 1734 cm^{-1} was probably due to Cu(II) and carboxylic groups bonding.

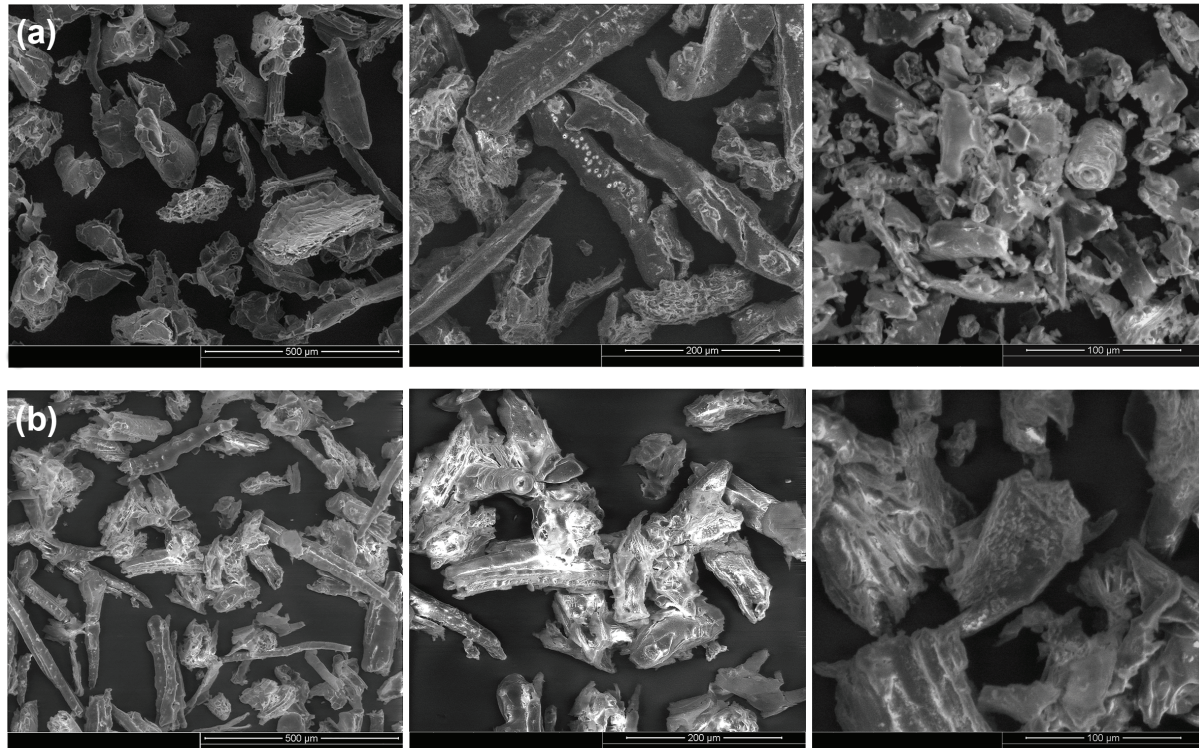


Figure 1. Images of PCP visualised by SEM: (a) Raw PCP; (b) PCP after Cu(II) adsorption.

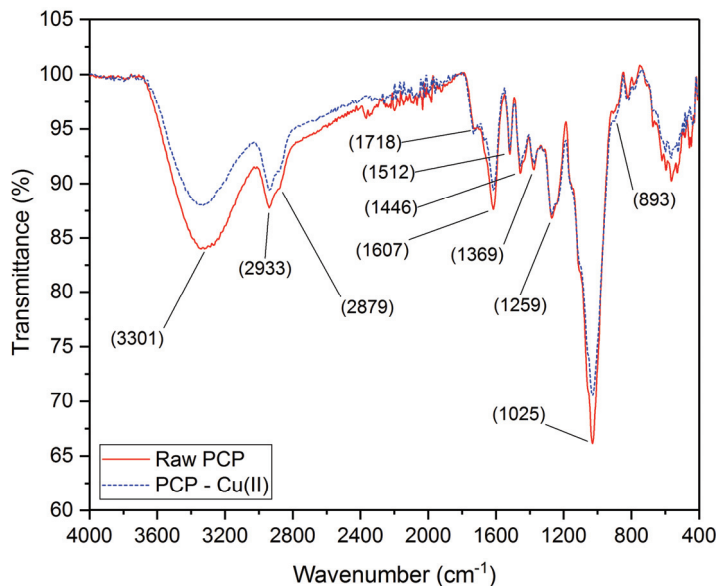


Figure 2. FTIR spectra of raw PCP and PCP after Cu(II) adsorption.

The alteration of the IR bands can be interpreted by their involvement in Cu(II) adsorption. This change is probably due to the interaction between these groups and Cu(II). The participation of the hydroxyl, carboxyl and phenolic groups in metal ions binding was reported in several studies [34-37].

XRD analysis

Figure 3 shows the diffractograms of raw PCP and PCP after Cu(II) adsorption. X-ray diffraction was used to study the effect of Cu(II) adsorption on the PCP cellulose crystallinity. The four peaks located at 2θ angles of 15.09, 16.25, 22.21 and 34.47° are characteristic of cellulose I [38,39].

The empirical crystallinity index (CrI) was estimated using the Segal equation [40] :

$$CrI (\%) = 100 \frac{I_c - I_{am}}{I_c} \quad (8)$$

where CrI expresses the relative degree of crystallinity, I_c is the intensity of the diffraction at $2\theta = 22.21^\circ$ and I_{am} referring to the intensity at $2\theta = 18.28^\circ$ assigned to the amorphous cellulose phase which corresponds to the minimum position of the diffraction profile.

The calculated crystallinity index of the cellulose shows a slight decrease in crystallinity from approx-

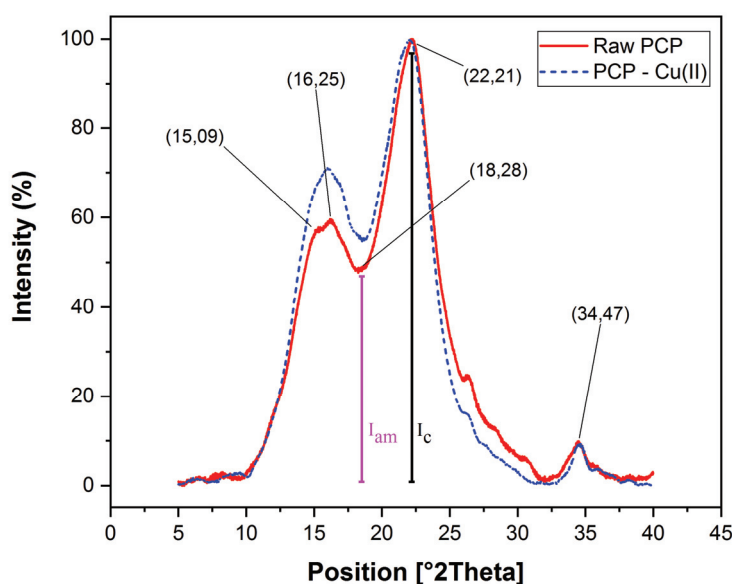


Figure 3. XRD of raw PCP and PCP after Cu(II) adsorption.

imately 51.32 to 45.10% when the adsorption of Cu(II) occurs. The results of XRD analysis suggest that the cellulose is involved in the adsorption of Cu(II) on the PCP.

Thermogravimetric analysis

Figure 4 presents the TGA and DTG profiles of PCP, the TGA measurements revealed three stages of the decomposition process: water evaporation (40–175 °C), removal of volatile organic matters (175–400 °C), and combustion of carbonaceous matter (400–645 °C). The temperature of the maximum mass loss rate can be determined by DTG, they are 79, 342 and 456 °C for the first, the second and the third stage, respectively. The processes of thermal destruction of PCP proceeded with maximum rate at 342 °C under air atmosphere.

The specific surface area of the material was found to be 0.76 m² g⁻¹ (Table 1), it's similar to that of sawdust of walnut 0.72 m² g⁻¹ [41] and peanut hulls 0.57–0.01 m² g⁻¹ [42]. The latter has a maximum adsorption capacity equal to 14.13 mg g⁻¹ for Cu(II).

Table 1. Some characteristic properties of PCP

Sample	pH _{pzc}	S _{BET} (m ² g ⁻¹)	pH _{adsorbent}	EC (μS cm ⁻¹)
PCP	5.62	0.76	5.30	441

Adsorption kinetics study

The effect of contact time on the adsorption of Cu(II) by PCP was shown in Figure 5. Evidently, the Cu(II) adsorption capacity increased with contact time until it reached a maximum value of 2.53 mg g⁻¹ at 60 min and remained constant over time. Contact time of

60 min was assumed appropriate for subsequent experiments, in which case the adsorption equilibrium could be reached. Similar results were reported using spruce sawdust [44].

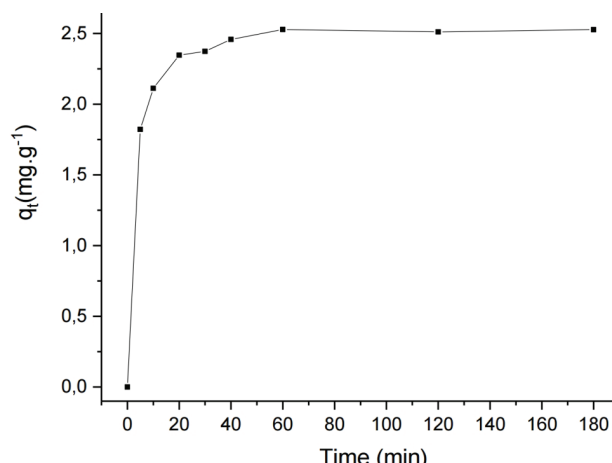


Figure 5. Effect of time on Cu(II) adsorption by PCP.

Due to the large number of active adsorbent sites accessible for metal adsorption, the rate of Cu(II) removal was higher at the beginning. As the competition for the availability of active sites intensifies by the metal ions remaining in the solution, the metal uptake by the PCP surface slowed down. After 60 min, the surface pores of adsorbents may be covered and it becomes difficult for Cu(II) to enter into the interior of the pores. Ofomaja *et al.* [39] reported that Cu(II) adsorption by cone powder became almost constant after 15 min. On the other hand, Değirmen *et al.* [18] reported an equilibrium time about 120 min.

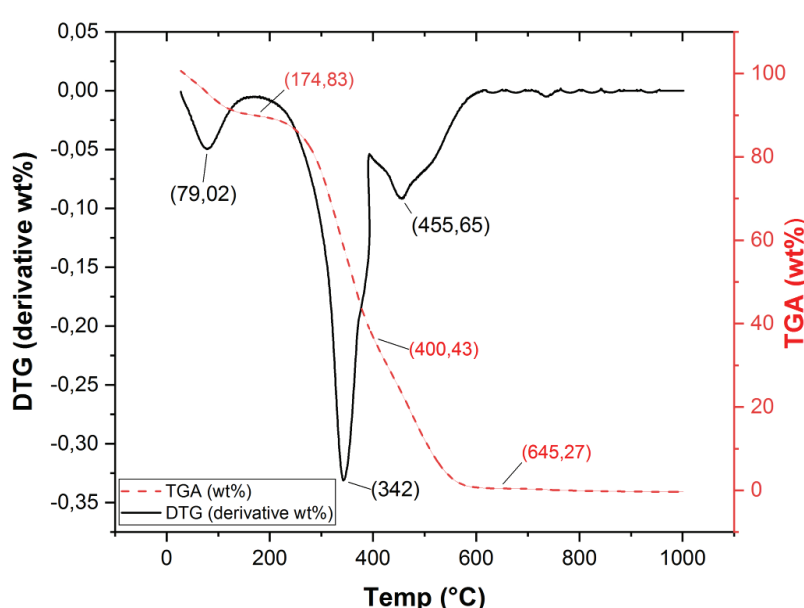


Figure 4. Thermogravimetric analysis (TGA) and derivative thermogravimetry (DTG) profiles of PCP.

Kinetic adsorption models

The study of adsorption kinetic describes the solute uptake rate, which controls the residence time of adsorbate uptake at the solid-solution interface including the diffusion process.

The pseudo-first order equation (Eq. (9)) can be expressed in nonlinear (Eq. (10)) and linear forms (Eq. (11) or Eq. (12)):

$$\frac{dq_t}{dt} = k_1(q_e - q_t) \quad (9)$$

$$q_t = q_e(1 - e^{-k_1 t}) \quad (10)$$

$$\log(q_e - q_t) = \log q_e - \frac{k_1}{2.303} t \quad (11)$$

$$\ln(q_e - q_t) = \ln q_e - k_1 t \quad (12)$$

Eq. (10) is known as PFO kinetic adsorption model, where q_t is the amount of adsorbate adsorbed at time t (mg g^{-1}) and can be calculated using Eq. (1), q_e is the equilibrium adsorption capacity (mg g^{-1}), k_1 is the PFO rate constant (min^{-1}), and t is the contact time (min).

The integration of PSO equation (Eq. (13)) with initial conditions leads to Eq. (14), which is known as PSO kinetic adsorption model:

$$\frac{dq_t}{dt} = k_2(q_e - q_t)^2 \quad (13)$$

$$q_t = \frac{q_e^2 k_2 t}{1 + k_2 q_e t} \quad (14)$$

PSO kinetic adsorption model can be expressed in the following linear form:

$$\frac{t}{q_t} = \frac{1}{k_2 q_e^2} + \left(\frac{1}{q_e} \right) t \quad (15)$$

where k_2 ($\text{g mg}^{-1} \text{ min}^{-1}$) is the PSO rate constant.

The plot of $\ln(q_e - q_t)$ versus t gives a straight line for the pseudo-first adsorption kinetic, which allows the determination of k_1 from the slope and q_e from y -intercept. For the second order adsorption kinetic, q_e and k_2 can be determined from the intercept of the linearised plot of $1/q_t$ versus t .

The Elovich equation can be expressed mathematically as follows:

$$q_t = \frac{1}{\beta} \ln(1 + \alpha \beta t) \quad (16)$$

where α is the initial rate constant ($\text{mg g}^{-1} \text{ min}^{-1}$) and β (mg g^{-1}) is the desorption constant at time.

The intraparticle diffusion model can be described by the following equation:

$$q_t = K_{int} t^{1/2} + C \quad (17)$$

where K_{int} is the intraparticle diffusion model rate constant ($\text{mg g}^{-1} \text{ min}^{1/2}$), which can be evaluated from the slope of the linear plot of q_t versus $t^{1/2}$. C (mg g^{-1}) is the constant related to the thickness of the boundary layer. Extrapolation of the linear portions of the plots back to the y -axis gives the intercepts, which provide the measure of the boundary layer. A higher value of C corresponds to a greater boundary layer effect.

The kinetic parameters in Eqs. (12) and (15) could be derived from the slopes and intercepts of the fitted curves shown in Figure 6b and a, respectively.

The calculated kinetic constants and their corresponding error function values are given in Table 2. Figure 6b shows the experimental data fitted to the linear PFO kinetic model; poor linearity was perceived for the PFO linear model with $R^2 = 0.89$ and $R_{adj}^2 = 0.87$. Additionally, the calculated adsorption at equilibrium ($q_{e,cal} = 1.32 \text{ mg g}^{-1}$) is underestimated when compared to the experimental equilibrium adsorption capacity ($q_{e,exp} = 2.53 \text{ mg g}^{-1}$). Accordingly, the linear PFO model was inadequate to describe the kinetic behaviour of Cu(II) adsorption by PCP.

The PSO kinetic model presented in Figure 6a gives a value of $R^2 = 1$ and $R_{adj}^2 = 1$. The calculated adsorption at equilibrium (2.55 mg g^{-1}) is much closer to the experimental value. These results indicate that the adsorption process was successfully represented by PSO model. Such findings support the assumption that the rate-limiting step of Cu(II) adsorption by PCP could be chemisorption involving valence forces through sharing or exchange of electrons between adsorbate and adsorbents [45]. According to the literature data, the PSO model was well applied to the adsorption of metal ions, dyes, and organic substances from aqueous solutions onto a wide range of adsorbents [18,46,47].

The intraparticle diffusion model is presented in Figure 6d. The plot of q_t versus $t^{1/2}$ gives multiple linear regions indicating that the adsorption process is governed by a multistep mechanism.

The first stage, with a higher slope, represents the transport in the solution phase, known as bulk transport, which takes place instantaneously after the adsorbent is transferred into the adsorbate solution; usually, this stage is too fast for agitated systems.

Then follows the second gradual adsorption stage, due to the film diffusion effects. In this stage,

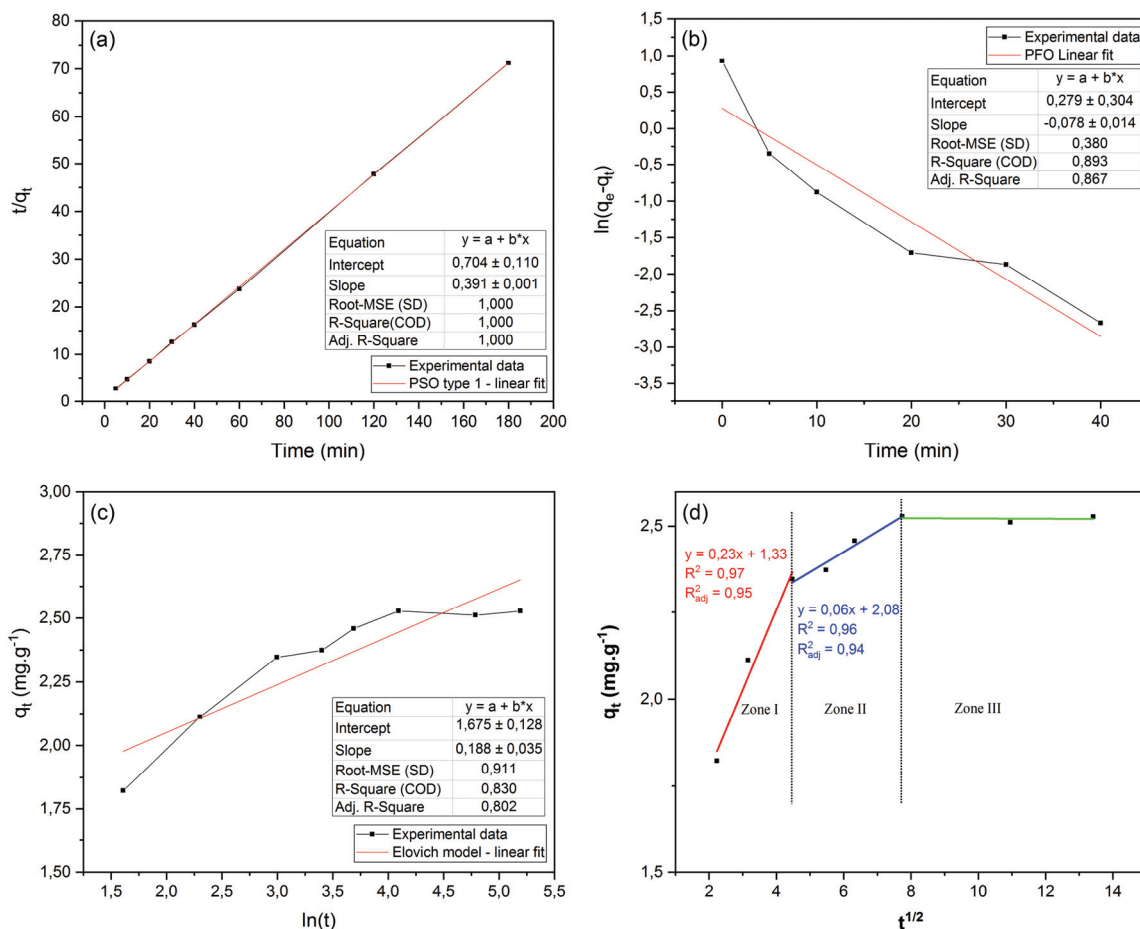


Figure 6. Kinetic model plots for Cu(II) adsorption by PCP: a) pseudo-second order; b) pseudo-first order; c) Elovich; d) intraparticle diffusion.

Table 2. Pseudo-first order, pseudo-second order and Elovich kinetics parameters for the adsorption of Cu(II) by PCP

Pseudo-first-order				
k_1 (min ⁻¹)	$q_{e,cal}$ (mg g ⁻¹)	$q_{e,exp}$ (mg g ⁻¹)	R^2	R_{adj}^2
0.078	1.322	2.528	0.893	0.867
Pseudo-second-order				
k_2 (g mg ⁻¹ min ⁻¹)	$q_{e,cal}$ (mg g ⁻¹)	$q_{e,exp}$ (mg g ⁻¹)	R^2	R_{adj}^2
0.218	2.555	2.528	1.000	1.000
Elovich				
β (mg g ⁻¹)	α (mg g ⁻¹ min ⁻¹)	R^2	R_{adj}^2	β (mg g ⁻¹)
5.315	1380.467	0.830	0.802	5.315

the heavy metals are transported from the solution to the adsorbent's external surface.

After saturation of the surface, the third straight stage involves the intraparticle diffusion through pore and interior surface of the PCP until the equilibrium between the metal ions in the solution and on the adsorbent surface is reached. Several previous investigations have reported a similar type of pattern [31,41,47].

According to this model, if only intraparticle scattering is involved in the process, the line passes through the origin, which is not the case in this study implying that intraparticle scattering is not the only one that controls the rate of adsorption of Cu(II) by PCP. From the slope of the linear portion of the second zone it was possible to determine k_{io} which is 0.06 mg g⁻¹ min^{-0.5} [28].

The Elovich kinetic model presented in Figure 6c gives a value of $R^2 = 0.83$ and $R_{adj}^2 = 0.80$, which

is lower than PSO and PFO models. The Elovich equation describes mainly chemisorption kinetic on systems with heterogeneous adsorbent surfaces [31].

Effects of adsorption parameters

Effect of pH

The effect of the pH solution was carried out by varying the initial pH of solutions from 2 to 8 (Figure 7a). A low adsorption capacity was observed at strong acidic medium. Also, it is remarkable that the adsorption capacity of PCP tends to increase with increasing pH value. The effect of pH can be interpreted by a decrease in the competition of positively charged species including H^+ , H_3O^+ and Cu^{2+} for the same adsorption sites. As the pH value was increased, more active sites were exposed and the number of negatively charged groups on the adsorbent matrix probably increased, enhancing the Cu(II) removal. In addition, it was observed that the optimum Cu(II) removal occurred between the pH values of 5 and 6. At pH solution higher than 6, precipitation of Cu(II) as copper hydroxides $Cu(OH)_2$ begins taking place, restricting the adsorption study. These findings

are in agreement with results reported in the previous studies [49,50].

The effect of pH could also be explained by considering pH_{pzc} presented in Table 1. It was observed a rise and fall of % of Cu(II) removal at $pH > pH_{pzc}$ and $pH < pH_{pzc}$, respectively. These observations could be explained by the fact that the adsorbent surface is positively charged for $pH < 5.62$ and it becomes negatively charged for $pH > 5.62$. At pH below 5.62, the adsorption is unfavourable because of repulsive electrostatic interactions between metal ions and positively charged functional groups. The maximum adsorption of Cu(II) occurs at pH values between 5 and 6 when the adsorbent surface is negatively highly charged.

It is noteworthy that Cu^{2+} , $Cu(OH)^+$ and $Cu(OH)_2$ are the dominant species involved in the adsorption below pH 5.3. Thus, Cu^{2+} and $Cu(OH)^+$ species may be adsorbed at the surface of PCP by ion exchange mechanism, while $Cu(OH)_2$ are accounted in the formation of hydrogen bonding with the -COOH and -OH functional groups present in PCP [48,50].

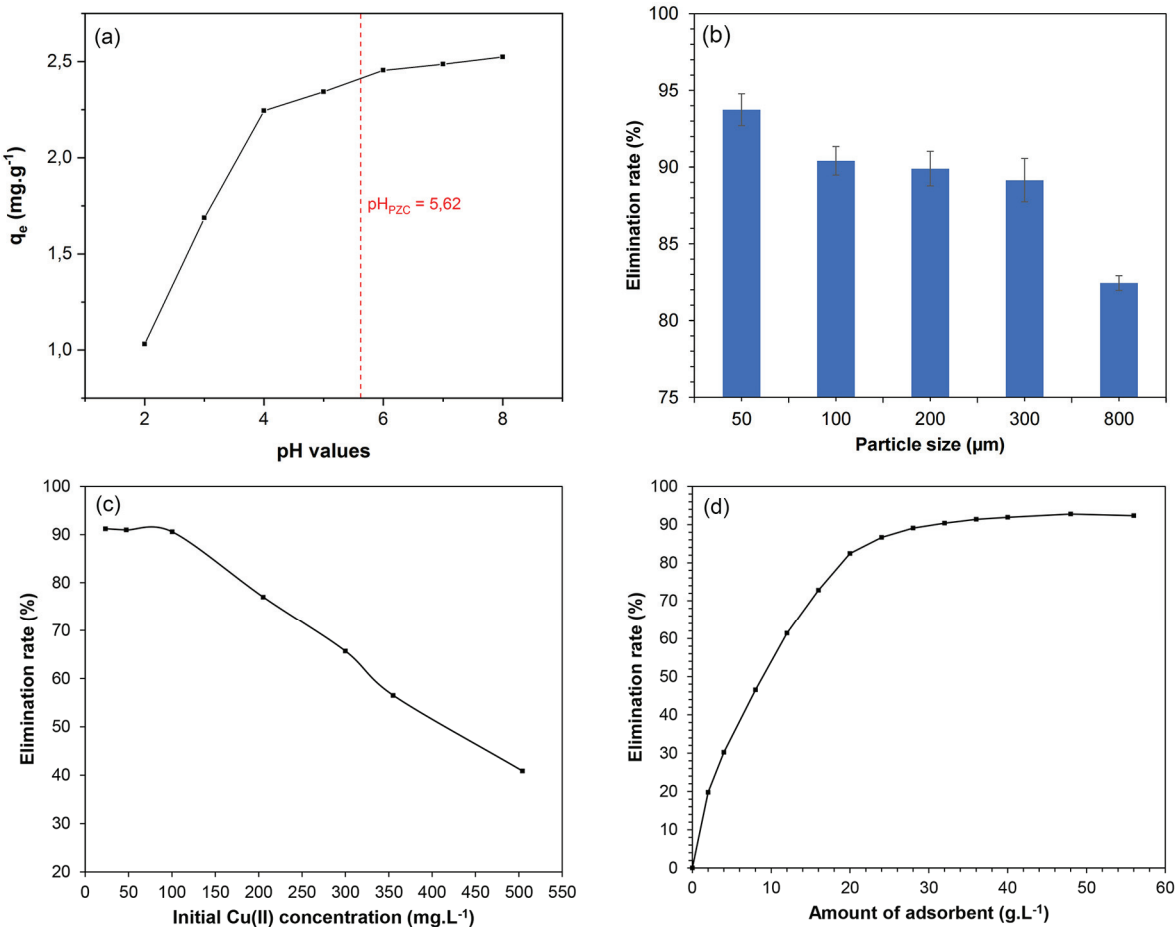
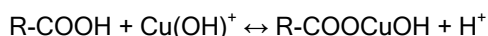
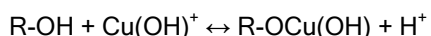
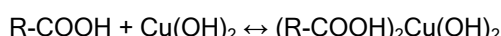
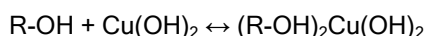


Figure 7. Effect of Cu(II) adsorption parameters by PCP: a) pH; b) particle size; c) initial Cu(II) concentration; d) adsorbent dose.

Ion exchange mechanism:



Hydrogen bonding mechanism:



The pH of the solution is one of the most critical parameters governing the metal adsorption process. It is correlated with the competition ability of hydrogen ions with metal ions to active sites on the PCP surface [48]. The FTIR spectroscopic analysis showed that the PCP has a variety of functional groups such as carboxyl, hydroxyl and amine. These groups are involved in almost all potential binding mechanisms.

Effect of adsorbent dose

Figure 7d shows that the percentage removal of Cu(II) increases with the increase in the adsorbent dose from 2 to 36 g L⁻¹; further increase of the adsorbent dose did not provide a significant rise in the percentage of the metal ion removed. Such behaviour was expected due to the saturation level attained during the adsorption process. The maximum elimination rate of Cu(II) was found to be 91% at PCP concentration of 36 g L⁻¹.

This result can be explained by the fact that the increase of the PCP dose provides more binding sites. Thus, leading to the enhancement of Cu(II) uptake. A similar effect of adsorbent dose was reported in the previous studies [17,18].

Effect of adsorbent particle size

The percentage removal of Cu(II) at different particle size presented in Figure 7a showed that a decreasing in the particle size leads to an increase in the adsorption efficiency. Particle sizes smaller than 100 µm were found to yield highest percentage removal of Cu(II). The higher adsorption level achieved by smaller particle sizes of the adsorbent may be related to the fact that smaller particles give large surface areas. Indeed, there is a tendency that smaller particles have more accessible surface for metal ions uptake [42].

Effect of initial Cu(II) concentration

The effect of metal concentration on the percent removal of Cu(II) shown in Figure 7c, revealed that the percentage of metal removal decreased with the increase of the initial Cu(II) concentration. At lower Cu(II) concentrations, the elimination rate was higher

due to the large number of active sites available for Cu(II) adsorption. While at a higher initial Cu(II) concentration, the active sites are saturated and the ratio of the initial number of Cu(II) to the available adsorption surface area was higher. As a result, the Cu(II) elimination percentage decreases. The lower adsorption percentages at higher Cu(II) concentrations might be associated with insufficient binding sites for adsorption or to the saturation of the binding sites. A similar effect of the initial metal ions concentration on the adsorption of Cu(II) by pine cone shells was found by Değirmen *et al.* [18].

Adsorption isotherms

Langmuir model

The Langmuir isotherm was developed by assuming that the adsorption happens at a specific number of accessible sites on the adsorbent surface. All adsorption sites involved have the same energy. The adsorption is monolayer, reversible and maximum adsorption occurs when adsorbed molecules form a saturated layer on the surface of adsorbent [51].

The nonlinear expression of the Langmuir isotherm model is given as:

$$q_e = \frac{q_{\max} K_L C_e}{1 + K_L C_e} \quad (18)$$

where q_{\max} is the maximum saturated monolayer adsorption capacity (mg g⁻¹) and K_L is the Langmuir constant (L mg⁻¹) related to energy of adsorption which quantitatively reflects the affinity of binding sites.

The Langmuir model can be expressed in terms of a constant known as separation factor or equilibrium parameter (R_L) given by the following equation [52]:

$$R_L = \frac{1}{1 + K_L C_0} \quad (19)$$

R_L value indicates the adsorption nature to be either unfavourable ($R_L > 1$), linear ($R_L = 1$), favourable ($0 < R_L < 1$) or irreversible ($R_L = 0$) [31,53].

Freundlich model

The Freundlich isotherm model suggests that molecules are adsorbed as a monomolecular layer or multilayer on heterogeneous adsorbent surfaces and there is an interaction between the adsorbed molecules. Freundlich isotherm is suitable in treating metal ions adsorption at high concentrations. The non-linear expression of the Freundlich isotherm model is given as [25]:

$$q_e = K_F C_e^n \quad (20)$$

where K_F (mg g^{-1}) $(\text{L mg}^{-1})^{1/n}$ is the Freundlich constant and n (dimensionless) is the Freundlich intensity parameter, which indicates the magnitude of the adsorption driving force or the surface heterogeneity [54].

Redlich-Peterson model

The Redlich-Peterson isotherm was proposed upon considering the limitations of the Freundlich and Langmuir isotherms. This model incorporates the features of the Freundlich and Langmuir models, and it might be applicable for demonstrating adsorption equilibrium over a wide range of adsorbate concentrations. The nonlinear form of this empirical model is given as follows:

$$q_e = \frac{K_{RP}C_e}{1 + a_{RP}C_e^g} \quad (21)$$

where K_{RP} (L g^{-1}) and a_{RP} (mg L^{-1}) $^{-g}$ are the Redlich-Peterson constants and g (dimensionless) is an exponent whose value is limited to ≤ 1 .

Eq. (21) reduces to the Langmuir isotherm when $g = 1$, and transforms into the Freundlich isotherm when $a_{RP} \gg 1$ and $g = 1$.

Dubinin-Radushkevich model

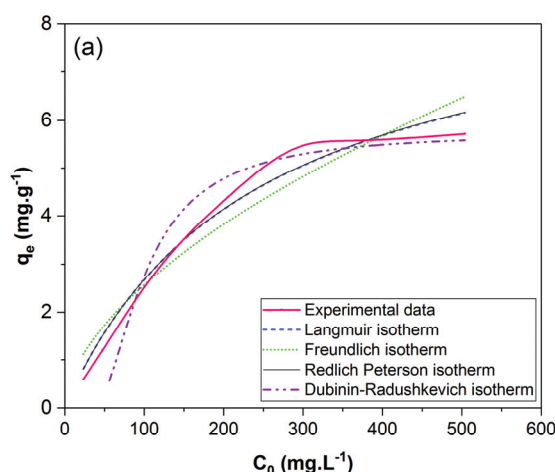
The Dubinin-Radushkevich equation was developed to express the adsorption isotherms in micropores. It is expressed as follows [31]:

$$q_e = q_{DR}e^{-K_{DR}\varepsilon^2} \quad (22)$$

ε is the Polanyi potential expressed as follows:

$$\varepsilon = R\bar{T}\ln\left(1 + \frac{1}{C_e}\right) \quad (23)$$

where q_{DR} (mg g^{-1}) is the adsorption capacity, K_{DR} ($\text{mol}^2 \text{ kJ}^{-2}$) is a constant related to the sorption energy,



R is the gas constant, T is the temperature in K, and q_e and C_e are obtained from Eq. (2).

The mean adsorption energy E (kJ mol^{-1}) can be obtained using:

$$E = \frac{1}{\sqrt{2K_{DR}}} \quad (24)$$

The isotherms using Langmuir, Freundlich, Redlich-Peterson and Dubinin-Radushkevich models are presented in Figure 8. The parameters of the models are listed in Table 3. The values of $R^2 = 0.98$ and $R_{adj}^2 = 0.97$ indicated that the Langmuir model yielded better fits compared to the other models. Therefore, Cu(II) bonding may occur on a homogenous surface under monolayer adsorption by energetically identical sites. In addition, the R_L values obtained using Eq. (19) are greater than zero and smaller than unity, indicating favourable adsorption of Cu(II) by PCP.

The value of adsorption energy obtained using Dubinin-Radushkevich Eq. (24) gives the nature of the adsorption of Cu(II) by PCP. A physical adsorption is obtained for $E < 8 \text{ kJ mol}^{-1}$ and chemical adsorption for $E > 8-16 \text{ kJ mol}^{-1}$ [30,55]. The E value ($20.31 \text{ kJ mol}^{-1}$) indicates that the removal of Cu(II) may occur through chemisorption uptake based on the ion exchange mechanism.

Table 4 presents the comparison of adsorption capacities of various adsorbents for Cu(II). The maximum adsorption capacity of Cu(II) by PCP reached a value of 9.08 mg g^{-1} , higher than that used by Blázquez *et al.* [17] and lower than that used by Değirmen *et al.* [18]. When it is opposed to other investigated raw waste materials, it is clearly visible that the PCP has a good adsorbent characteristic. These findings show that PCP may be used successfully for the removal of Cu(II) from aqueous solution.

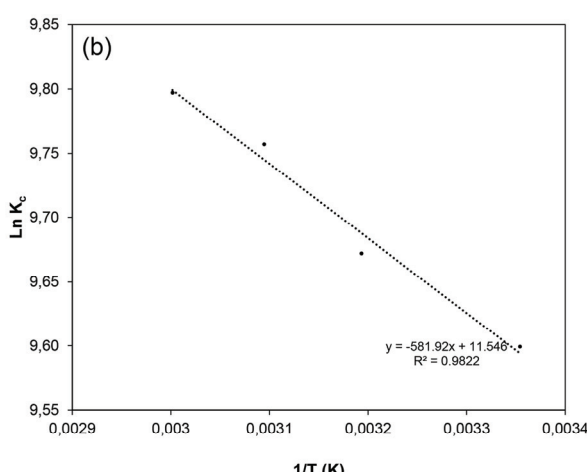


Figure 8. Cu(II) adsorption by PCP: a) isotherm fitting of Langmuir, Freundlich, Redlich-Peterson and Dubinin-Radushkevich models; b) Van 't Hoff plot for calculation of thermodynamic parameters.

Table 3. Isotherm parameters of Cu(II) adsorption by PCP deduced with nonlinear method

Model	Equation	Parameter	Value	Standard Error	Statistics	Value
Langmuir	$q_e = \frac{q_{\max} K_L C_e}{1 + K_L C_e}$	q_{\max} (mg g ⁻¹)	9.080	1.068	R_{adj}^2	0.975
		K_L (L mg ⁻¹)	0.004	0.001	R^2	0.979
		R_L (range) = 0.911 - 0.322				
Freundlich	$q_e = K_F C_e^n$	K_F (mg g ⁻¹) (L mg ⁻¹) ^{1/n}	0.183	0.103	R_{adj}^2	0.935
		n	1.740	0.300	R^2	0.922
Redlich-Peterson	$q_e = \frac{K_{RP} C_e}{1 + a_{RP} C_e^g}$	K_{RP} (L g ⁻¹)	0.038	0.015	R_{adj}^2	0.969
		a_{RP} (mg L ⁻¹) ^g	0.004	0.013	R^2	0.979
		g	1.000	0.434		
Dubinin-Radushkevich	$q_e = q_{DR} e^{-K_{DR} e^2}$	q_{DR} (mg g ⁻¹)	5.751	0.364	R_{adj}^2	0.932
		K_{DR} (mol ² kJ ⁻²)	0.0012	0.0004	R^2	0.943
		E (kJ mol ⁻¹)	20.315			

Table 4. Comparison of Cu(II) adsorption studies using various adsorbents

Adsorbent	Adsorption capacity (mg g ⁻¹)	Reference
Raw corn silk	15.35 (39.85 °C/pH 5.0)	[34]
Wheat straw	5 (pH and temperature N/S)	[58]
Apricot stones	5.90 (25 °C/pH 4.5)	[59]
Maple sawdust	9.19 (23 °C/pH 6.0)	[50]
Pine tree cones	19.27 (30 °C/pH 5.0)	[18]
Pine cone shells	6.81 (25 °C/pH 5.0)	[17]
Pine cone powder	9.08 (25 °C/pH 5.3)	This study

Thermodynamic study

The values of ΔG (kJ mol⁻¹) are directly calculated from Eq. (4), while the values of ΔH (kJ mol⁻¹) and ΔS (J mol⁻¹ K⁻¹) were evaluated from the intercept of the plot of $\ln K_c$ versus $1/T$ from the Van't Hoff equation (Eq. (6)) [34].

The calculated thermodynamic parameters are presented in Table 5. The negative values of ΔG indicated that adsorption is spontaneous and thermodyn-

energy. Endothermic adsorption of Cu(II) was reported by other authors for corn silk, bentonite and sewage sludge [34,56,57].

CONCLUSION

This research was focused on the adsorption of Cu(II) ions by PCP from aqueous solution. Characterisation confirmed the role of hydroxyl, carboxyl and phenolic groups in metal binding. The adsorption of the Cu(II) by PCP reached equilibrium in 60 min. The kinetic data showed that the pseudo-second-order kinetic model describes the adsorption of Cu(II) ions by PCP. The maximum adsorption efficiency of Cu (II) by PCP was found to be almost 91% at PCP dose of 36 g L⁻¹ with a Cu(II) concentration of 100 mg L⁻¹. Particle sizes smaller than 100 µm were found to yield the highest percentage removal of Cu(II). The optimum Cu(II) removal occurred at a slightly acidic pH. Adsorption equilibrium data fitted very well the Langmuir model. The maximum Cu(II) adsorption capacity (q_{\max}) obtained was 9.08 mg g⁻¹. The separation factor

Table 5. Thermodynamic parameters values of Cu(II) adsorption by PCP

T(K)	ΔG (kJ mol ⁻¹)	ΔH (kJ mol ⁻¹)	ΔS (J mol ⁻¹ K ⁻¹)	Van't Hoff equation
298.15	-23.80	4.84	96.00	$y = -581.92x + 11.55$
313.15	-25.18			$R^2 = 0.98$
323.15	-26.22			
333.15	-27.14			

amically favourable. The positive value of ΔS reflects the affinity of the Cu(II) towards the PCP adsorbent. It indicates the increase of the disorder at the solid/liquid interface during the adsorption. The positive value of ΔH indicated that the adsorption of Cu(II) is endothermic. It suggests that transferring Cu(II) from the aqueous phase to the solid phase requires

indicated a favourable adsorption of Cu(II) by PCP. The thermodynamic study showed that the Cu(II) adsorption was a spontaneous and endothermic process. The positive value of ΔS revealed the increase in the randomness at solid solution interface. PCP can be considered as a promising material for the removal of

Cu(II) from wastewater. It is readily available, low cost and above all, environmentally friendly.

REFERENCES

- [1] M.A.A. Wijayawardena, M. Megharaj, R. Naidu, in: *Adv. Agron.*, Elsevier Inc., 2016, pp. 175-234
- [2] M. Mahurpawar, *Int. J. Researh-Granthaalayah* 2350 (2015) 2394-3629
- [3] R. Ouafi, Z. Rais, M. Taleb, M. Benabbou, M. Asri, in: O.K. Stefan E (Ed.), *Sawdust Prop. Potential Uses Hazards*, Nova Science Publishers, Incorporated, 2017, pp. 147-181
- [4] S. Babel, T.A. Kurniawan, *J. Hazard. Mater.* 97 (2003) 219-243
- [5] C. Palma, E. Contreras, J. Urrea, M.J. Martínez, *Waste Biomass Valorization* 2 (2011) 77-86
- [6] M.T. Islam, R. Saenz-Arana, C. Hernandez, T. Guinto, M.A. Ahsan, D.T. Bragg, H. Wang, B. Alvarado-Tenorio, J.C. Noveron, *J. Environ. Chem. Eng.* 6 (2018) 3070-3082
- [7] M.T. Islam, C. Hernandez, M.A. Ahsan, A. Pardo, H. Wang, J.C. Noveron, *J. Environ. Chem. Eng.* 5 (2017) 5270-5279
- [8] C.K. Jain, D.S. Malik, A.K. Yadav, *Environ. Process.* 3 (2016) 495-523
- [9] N.S. Kumar, M. Asif, A.M. Poulose, M. Suguna, M.I. Al-Hazza, *Processes* 7 (2019)
- [10] A.E. Ofomaja, E.B. Naidoo, S.J. Modise, *Desalination* 251 (2010) 112-122
- [11] N.S. Kumar, M. Asif, M.I. Al-Hazzaa, *Environ. Sci. Pollut. Res.* 25 (2018) 21949-21960
- [12] G.M.A. Bouchair Abdennour, Bouremmad Farida, Shawuti Shalima, Amayreh Mousa Y, *Res. J. Chem. Environ.* 23 (2019) 10-18
- [13] A.I. Almendros, M.A. Martín-Lara, A. Ronda, A. Pérez, G. Blázquez, M. Calero, *Bioresour. Technol.* 196 (2015) 406-412
- [14] H. Ucun, Y.K. Bayhan, Y. Kaya, A. Cakici, O. Faruk Algur, *Bioresour. Technol.* 85 (2002) 155-158
- [15] D. Politi, D. Sidiras, *Procedia Eng.* 42 (2012) 1969-1982
- [16] A.E. Ofomaja, E.B. Naidoo, S.J. Modise, *J. Hazard. Mater.* 168 (2009) 909-917
- [17] G. Blázquez, M.A. Martín-Lara, E. Dionisio-Ruiz, G. Tenorio, M. Calero, *J. Ind. Eng. Chem.* 18 (2012) 1741-1750
- [18] G. Değirmen, M. Kılıç, Ö. Çepelioğullar, A.E. Pütün, *Water Sci. Technol.* 66 (2012) 564-572
- [19] R. Ouafi, Z. Rais, M. Taleb, *Desalin Water Treat.* 180 (2020) 185-192
- [20] S.K. Lagergren, *Sven. Vetenskapsakad. Handingarl.* 24 (1898) 1-39
- [21] G. Blanchard, M. Maunaye, G. Martin, *Water Res.* 18 (1984) 1501-1507
- [22] W.J. Weber, J.C. Morris, *J. Sanit. Eng. Div.* 89 (1963) 31-60
- [23] J. Zeldowitsch, *Acta Physicochim. URSS* 1 (1934) 364-449
- [24] I. Langmuir, *J. Am. Chem. Soc.* 40 (1918) 1361-1403
- [25] H. Freundlich, *Zeitschrift Phys. Chemie* 57 (1906) 386-470
- [26] M.M. Dubinin, in: *Dokl. Akad. Nauk SSSR*, 1947, pp. 327-329
- [27] O. Redlich, D.L. Peterson, *J. Phys. Chem.* 63 (1959) 1024-1024
- [28] É.C. Lima, M.A. Adebayo, F.M. Machado, in: C.P. Bergmann, F.M. Machado (Eds.), *Carbon Nanomater. as Adsorbents Environ. Biol. Appl.*, Springer International Publishing, Cham, 2015, pp. 33-69
- [29] S.K. Bozbash, Y. Boz, *Process Saf. Environ. Prot.* 103 (2016) 144-152
- [30] H.N. Tran, S.J. You, H.P. Chao, *J. Environ. Chem. Eng.* 4 (2016) 2671-2682
- [31] H.N. Tran, S.-J. You, A. Hosseini-Bandegharaei, H.-P. Chao, *Water Res.* 120 (2017) 88-116
- [32] X. Zhou, X. Zhou, *Chem. Eng. Commun.* 201 (2014) 1459-1467
- [33] V.S. Munagapati, V. Yarramuthi, S.K. Nadavala, S.R. Alla, K. Abburi, *Chem. Eng. J.* 157 (2010) 357-365
- [34] M. Petrović, T. Šoštarić, M. Stojanović, J. Petrović, M. Mihajlović, A. Čosović, S. Stanković, *Ecol. Eng.* 99 (2017) 83-90
- [35] N. Ouazene, M.N. Sahmoune, *Int. J. Chem. React. Eng.* 8 (2010) 151
- [36] H.L. Ornaghi Júnior, Á. de G.O. Moraes, M. Poletto, A.J. Zattera, S.C. Amico, *Cellul. Chem. Technol. Cellul. Chem. Technol.* 50 (2016) 15-22
- [37] A.N. Kosasih, J. Febrianto, J. Sunarso, Y.H. Ju, N. Indraswati, S. Ismadji, *J. Hazard. Mater.* 180 (2010) 366-374
- [38] Y.L. Hsieh, in: *Cotton*, Elsevier, 2007, pp. 3-34
- [39] A.E. Ofomaja, E.B. Naidoo, *Chem. Eng. J.* 175 (2011) 260-270
- [40] L. Segal, J.J. Creely, A.E. Martin, C.M. Conrad, *Text. Res. J.* 29 (1959) 786-794
- [41] Y. Bulut, Z. Tez, *J. Environ. Sci.* 19 (2007) 160-166
- [42] R.M. Ali, H.A. Hamad, M.M. Hussein, G.F. Malash, *Ecol. Eng.* 91 (2016) 317-332
- [43] V. Fierro, V. Torné-Fernández, D. Montané, A. Celzard, *Microporous Mesoporous Mater.* 111 (2008) 276-284
- [44] Z. Kovacova, S. Demcak, M. Balintova, *Proceedings* 16 (2019) 52
- [45] P. SenthilKumar, S. Ramalingam, V. Sathyaselvabala, S.D. Kirupha, S. Sivanesan, *Desalination* 266 (2011) 63-71
- [46] D. Park, Y.-S. Yun, J.M. Park, *Biotechnol. Bioprocess Eng.* 15 (2010) 86-102
- [47] I. Morosanu, C. Teodosiu, C. Paduraru, D. Ibanescu, L. Tofan, *N. Biotechnol.* 39 (2017) 110-124
- [48] F. Bouhamed, Z. Elouear, J. Bouzid, *J. Taiwan Inst. Chem. Eng.* 43 (2012) 741-749
- [49] A.E. Ofomaja, E.I. Unuabonah, N.A. Oladoja, *Bioresour. Technol.* 101 (2010) 3844-3852

- [50] M.S. Rahman, M.R. Islam, *Chem. Eng. J.* 149 (2009) 273-280
- [51] S.A. Sadeek, N.A. Negm, H.H.H. Hefni, M.M. Abdel Wahab, *Int. J. Biol. Macromol.* 81 (2015) 400-409
- [52] K.R. Hall, L.C. Eagleton, A. Acrivos, T. Vermeulen, *Ind. Eng. Chem. Fundam.* 5 (1966) 212-223
- [53] A. Labidi, A.M. Salaberria, S.C.M. Fernandes, J. Labidi, M. Abderrabba, *J. Taiwan Inst. Chem. Eng.* 65 (2016) 140-148
- [54] E. Worch, in: *Adsorpt. Technol. Water Treat.*, DE GRUYTER, Berlin, 2012, pp. 41-76
- [55] S. Yildiz, *Ecol. Chem. Eng. S.* 24 (2017) 87-106
- [56] J. Li, J. Hu, G. Sheng, G. Zhao, Q. Huang, *Colloids Surfaces A Physicochem. Eng. Asp.* 349 (2009) 195-201
- [57] X. Wang, X. Liang, Y. Wang, X. Wang, M. Liu, D. Yin, S. Xia, J. Zhao, Y. Zhang, *Desalination* 278 (2011) 231-237
- [58] M. Gorgievski, D. Božić, V. Stanković, N. Šrbac, S. Šerbula, *Ecol. Eng.* 58 (2013) 113-122
- [59] M. Petrovic, T. Sostaric, L. Pezo, S. Stankovic, C. Lacnjevac, J. Milojkovic, M. Stojanovic, *Chem. Ind. Chem. Eng. Q.* 21 (2015) 249-259.

REDOUANE OUAIFI¹
ANASS OMOR¹
YOUNES GAGA²
MOHAMED AKHAZZANE¹
MUSTAPHA TALEB¹
ZAKIA RAIS¹

¹Engineering Laboratory of Organometallic, Molecular Materials and Environment, Faculty of Science Dhar El Mahraz, Sidi Mohamed Ben Abdellah University, Route d'immouzer, Fez, Morocco

²Laboratory of Biotechnology, Ecology and Preservation of Natural Resources, Faculty of Science, Dhar El Mahraz, Sidi Mohamed Ben Abdellah University, Route d'immouzer, Fez, Morocco

NAUČNI RAD

UKLANJANJE JONA BAKRA IZ VODE ADSORPCIJOM NA PRAHU BOROVIH ŠIŠARKI

U ovom radu istraživan je adsorpcioni potencijal prah borovih šišarki za uklanjanje jona bakra iz vodenih rastvora. Proces adsorpcije je bio relativno brz i završio se za 60 min. Kinetički model pseudo-drugog reda pravilno opisuje adsorpciju jona bakra pomoću praha borovih šišarki. Adsorbent je okarakterisan različitim instrumentalnim tehnikama i sprovedeni su šaržni eksperimenti da se istraži uticaj doze praha, pH rastvora, veličine čestica i početne koncentracije jona bakra na efikasnost adsorpcije. Optimalno uklanjanje jona bakra postignuto je pri blago kiselom pH, sa veličinom čestica manjim od 100 mm. Efektivna doza praha je procenjena na 36 g/l. Povećanje početne koncentracije jona bakra je praćeno smanjenjem brzine njihovog uklanjanja za skoro polovinu. Langmuirov model je bio najbolja izoterma sa maksimalnim kapacitetom adsorpcije od 9,08 mg/g. Vrednosti termodinamičkih parametara su pokazale da je adsorpcija jona bakra bio spontan i endotermni proces. Rezultati ovog istraživanja sugerisu da bi joni bakra mogli biti uklonjeni ekološki prihvatljivim procesom korišćenjem praha borovih šišarki kao jeftinog prirodnog otpada.

Ključne reči: uklanjanje jona bakra, izoterme, kinetika, prirodni otpad, prah šišarki, tretman.